

# Delineation of phase fields at the Te-rich end of the Ru–Te binary system

M. Ali (Basu), S.R. Bharadwaj, D. Das \*

*Applied Chemistry Division, Bhabha Atomic Research Centre, Trombay, Mumbai-400085, India*

Received 3 September 2004; accepted 25 November 2004

## Abstract

The tellurium rich side of the ruthenium–tellurium binary system was studied by differential thermal analysis. To avoid reported problems of Te loss by evaporation and reactive interference of Te to the thermocouples of the thermal analyzer, the present study made use of specially designed sealed quartz capsules as DTA containers. The thermal analyses were carried out over the compositional range of  $0.66 \leq x_{\text{Te}} \leq 1.00$  with the help of SETARAM TG/DTA and other indigenously built thermal analyzers available in this laboratory. The thermal data generated for fifteen different compositions were interpreted for the nature of phase transitions occurring at their characteristic temperatures. The Ru–Te binary system was found to have a eutectic transformation at 444 °C at a composition of  $x_{\text{Te}} = 0.918$  and a monotectic transformation at 447 °C at a composition of  $x_{\text{Te}} = 0.700$ . Up to 6 at.% Ru is soluble in Te at about 440 °C. © 2005 Elsevier B.V. All rights reserved.

## 1. Introduction

Ru is one of the constituents of the metallic precipitates of fission products that are collectively known as ‘white inclusions’ in irradiated fuel pins [1]. Although tellurium is generated in low yield (only 1.6 mass% of the fission products) [1], it is one of the active corrosion agents for the clad. Tellurium can remain dissolved in the oxide fuel [2], or depending on the local oxygen potential, it can be a constituent of fission product oxide phases or form metallic phases with Pd, Rh or Ru [3]. Delineation of the phase fields for intermetallic systems of the fission products is important in understanding the distribution of metallic components and tellurium in dif-

ferent phases. It also gives insight into the probable types of phases that are formed in glass matrix vitrification. For instance, although Ru gets oxidized and escapes as gaseous  $\text{RuO}_3$  and  $\text{RuO}_4$  species during the process of vitrification, evidence could be furnished on the existence of  $\text{Ru}_{1-x}\text{RhO}_2$  and Rh–Pd–U–Te–O precipitates [3] in vitrified waste.

The phase diagram of the Ru–Te binary system has been reported in the literature [4–7]. Detailed information is available on  $\text{RuTe}_2$ , which is known to be the only intermetallic compound formed in the system. The DTA studies reported in [7] were done with compositions only up to 70 at.% of Te. Above 70 at.% Te there is very little information on the nature of liquid phases of the system. Therefore, it is difficult to carry out thermal analysis on Te rich liquid where Te vaporization is significant and the vapor is aggressive to the thermopile probe used in the analysis. Since reliable phase diagram data in the Te-rich region are not available, this region

\* Corresponding author. Tel.: +91 22 5505151; fax: +91 22 5519613.

E-mail address: [dasd@apsara.barc.ernet.in](mailto:dasd@apsara.barc.ernet.in) (D. Das).

of the Ru–Te binary system was investigated in the present study. The phase fields of the compositional region covering the intermetallic phase RuTe<sub>2</sub> to pure Te were delineated within ambient temperature to 500 °C with the help of the thermal analysis technique after taking precautionary measures against Te attack with the DTA probe. The phase field delineation was further supported for some compositions by XRD analysis.

## 2. Experimental

### 2.1. DTA studies

Powders of pure Ru (Aldrich, 99.99% pure) and Te (Aldrich, 99.99% pure) were thoroughly mixed at different compositions ( $x_{\text{Te}} = 1.00, 0.987, 0.984, 0.969, 0.957, 0.950, 0.940, 0.918, 0.900, 0.850, 0.800, 0.750, 0.720, 0.700, 0.667$ ). The relatively Ru rich compositions ( $x_{\text{Te}} = 0.900$  to  $0.667$ ) were studied using a SETARAM simultaneous TG-DTA unit (model 92-16.18) and employing vacuum-sealed samples in quartz holders. These holders were built in conformity with the holder's stand of the TG-DTA unit. Usages of this unit for compositions of higher Te contents were restricted for possible damage of the thermopile probe by any accidental release of Te from the sealed sample holder. Thus the first eight Te-rich compositions were studied in the home-made DTA apparatus in which samples were contained in quartz holders under flowing Ar–8% $\text{H}_2$  mixture to prevent oxidation of Ru or Te. The DTA apparatus equipped with a microprocessor-based temperature controller cum programmer had chromel–alumel thermocouples for monitoring the sample temperature and the differential thermal signal. The details of the apparatus is described elsewhere [8].

The home-made and the SETARAM DTA apparatus were calibrated for temperature with the melting points of Sn (231.97 °C), Zn (419.5 °C), Te (449.5 °C) and TeO<sub>2</sub> (733 °C) in sealed silica crucibles under vacuum. The effect of reduced pressure inside the sealed crucible on the melting point being insignificant was not considered. For a few Te rich compositions including pure Te, thermal analyses were also carried out in a SETARAM-made unit for confirming the correspondence of their DTA results to those obtained using the home-made unit.

The DTA studies were carried out typically on  $\approx 500$  mg sample. The DTA run was first taken with pure Te. Subsequent compositions with decreasing Te contents ( $x_{\text{Te}} = 0.987, 0.984, 0.969, 0.957, 0.950, 0.940, 0.918$ ) were then prepared in-situ. In each case the sample was heated to 500 °C, which is about 50 °C above the melting temperature of Te and held there for 30 min for attainment of homogeneity. The attainment of spatial homogeneity was confirmed by metallographic examination on one of the annealed samples that was quickly

withdrawn out of the furnace under flowing Ar–8% $\text{H}_2$  mixture. The DTA runs of the annealed compositions were taken in the second heating cycle, which were recorded at 5 °C  $\text{min}^{-1}$ . The reproducibility of the DTA curve was confirmed for each sample over two thermal cycles between room temperature and 500 °C. Heating cycles have defined characteristic endothermic peaks due to phase transitions at different temperatures for a given composition. Significant under-cooling was observed in the cooling cycles. The remaining compositions ( $x_{\text{Te}} = 0.900$ – $0.667$ ) studied using the SETARAM simultaneous TG-DTA unit (model 92-16.18) were also given similar type of heat treatment as given for the previous

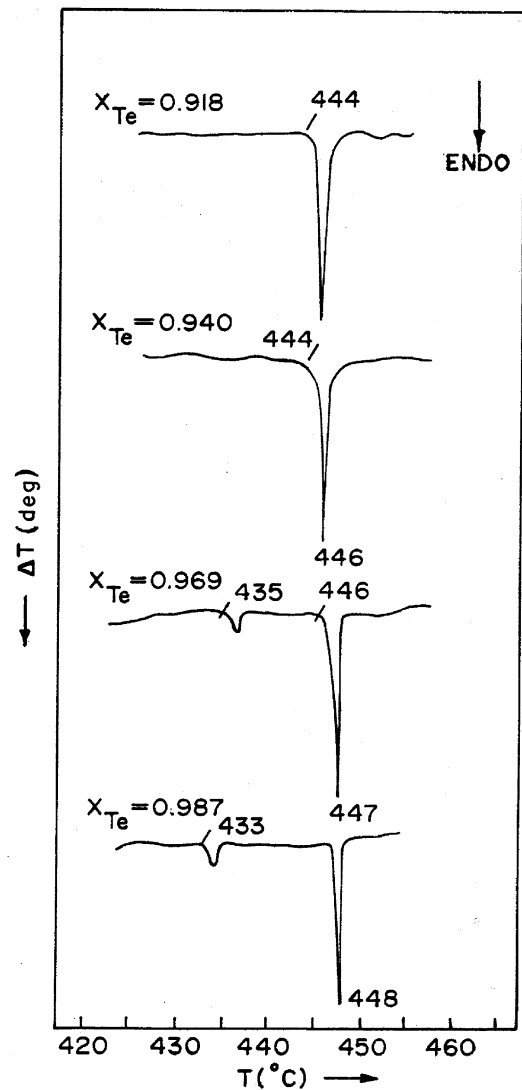


Fig. 1. Typical DTA curves obtained for compositions from  $x_{\text{Te}} = 0.918$  to  $0.987$  during heating.

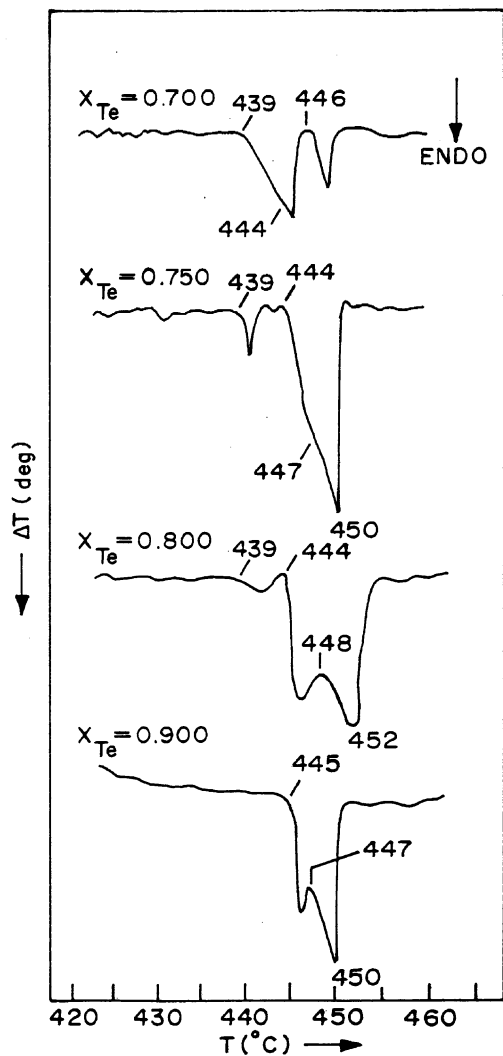


Fig. 2. Typical DTA curves obtained for compositions from  $x_{\text{Te}} = 0.70$  to  $0.90$  during heating.

group of samples. About 50 mg of sample was taken in for each composition in a sealed quartz holder. Typical thermal curves obtained in the different compositional regions are shown in Figs. 1 and 2.

### 2.2. Pyrometric studies

The intermetallic  $\text{RuTe}_2$  that reportedly [7] decompose above  $1175^\circ\text{C}$  was subjected to pyrometric observation to see whether a liquid phase appears before the decomposition. For this, pellet of  $\text{RuTe}_2$  placed in an alumina cup inside a molybdenum Knudsen cell was inductively heated ( $30\text{ kW} \times 450\text{ kHz}$  Lepel induction heater, USA) under high vacuum, and the focused image of cell orifice (1.5 mm diam.) over viewing the inside pel-

let was observed through a visual optical pyrometer (Leeds and Northrup, USA). To avoid a large loss of Te by evaporation during the experiment, the heating rate was kept high enough ( $100^\circ\text{C}/\text{min}$ ) to attain the cell temperature around  $1200^\circ\text{C}$  in a short time. Above this temperature the heating rate was kept lower for precise visual monitoring of color-temperature as well as for any optical change in the focused image of the cell orifice. It has been reported that due to sudden change in light reflectivity during melting and mirror effect of the molten sites, black spots sharply appear when the solidus point is reached and those spots converge to a single one at the liquidus point [9]. The pyrometer was pre-calibrated to an overall accuracy of  $5^\circ\text{C}$  at  $1500^\circ\text{C}$  using the reported method [10]. The transmittance of the observation window of the vacuum system was measured at 650 nm before and after the heating runs. After the experiment, the residue left inside the alumina cup was analyzed by XRD.

### 2.3. XRD studies

Room temperature XRD studies were carried out on high temperature-annealed compositions using a Philips diffractometer (PW 1729/40). High-temperature XRD studies could not be carried out due to the risk of attack of the exposed parts of the instrument by Te vapors.

### 2.4. Quenching studies

A quenching furnace with uniform temperature zone of 5 cm and temperature controlled to  $\pm 1^\circ\text{C}$  was used for annealing and then quenching experiments. A typical composition of  $x_{\text{Te}} = 0.80$  was sealed in a quartz ampoule and centrally located in the uniform zone of the furnace by a suspension wire. It was annealed at  $450^\circ\text{C}$  for 2 h and the suspension wire was snapped and the sample dropped instantaneously into liquid nitrogen. The sample was stored in liquid nitrogen till the preparation for XRD.

## 3. Results

Pure Te showed a single sharp peak at  $449^\circ\text{C}$ . The composition with  $x_{\text{Te}} = 0.987$  gave a small peak at  $433^\circ\text{C}$  and a large liquidus peak at  $448^\circ\text{C}$  (Fig. 1). At successive compositions of  $x_{\text{Te}} = 0.984, 0.969, 0.957$  and  $0.944$ , the nature of the smaller peak remains identical and it was observed at  $434, 435, 437$  and  $438^\circ\text{C}$ , respectively, for the cases. The more prominent liquidus peak was observed for these compositions at  $447, 447, 446$  and  $445^\circ\text{C}$ , respectively. One single asymmetric endotherm peak was observed at  $x_{\text{Te}} = 0.940$  with the onset at  $444^\circ\text{C}$  and the liquidus peak at  $446^\circ\text{C}$ . At

$x_{\text{Te}} = 0.918$ , a single symmetric peak was obtained at 444 °C which was assigned to be the eutectic temperature. At  $x_{\text{Te}} = 0.900$  two merged endotherms were observed at 445 °C and 447 °C, respectively. The second endotherm was asymmetric with the liquidus peak temperature at 450 °C. So the onset temperature of 447 °C probably indicated the beginning of a second transition (monotectic) after the eutectic (Fig. 2). There is one small peak at 439 °C for  $x_{\text{Te}} = 0.850$  due to the reported marcasite-to-pyrite phase transition of  $\text{RuTe}_2$  [6] followed by two merged endotherms at 443 and 447 °C due to the eutectic and monotectic, respectively. There is one small peak at 452 °C due to the liquidus. Four well resolved features were obtained for the composition of  $x_{\text{Te}} = 0.800$  at 439, 444, 448 and 452 °C corresponding to the  $m \rightarrow p$  phase transition, the eutectic, monotectic and the liquidus, respectively. The  $m \rightarrow p$  transition is a monotropic one as reported in [7]. Four similar DTA features were obtained for  $x_{\text{Te}} = 0.750$  at 439, 444, 447 and 450 °C. Three closely lying endotherms at 439, 444 and 447 °C were observed for  $x_{\text{Te}} = 0.720$ . This composition being closer to  $\text{RuTe}_2$  the first endotherm due to the  $m \rightarrow p$  transition is quite large. Three endotherms obtained at  $x_{\text{Te}} = 0.70$  are closely lying and observed at 439, 444 and 446 °C. The feature at 444 °C, which corresponds to the eutectic appeared as a shoulder to

the peak at 439 °C. No melting peak was observed up to 500 °C. The composition corresponding to the compound  $\text{RuTe}_2$  was also taken for DTA study. It showed one endotherm at 439 °C and no other peak up to 1000 °C. XRD analysis of the compositions,  $0.667 \leq x_{\text{Te}} \leq x_{\text{Te}} 0.850$ , that exhibited the endotherm at 439 °C due to the crystallographic transition showed indeed the presence of pure Te and a mixture of  $m$ - and  $p$ -phases of  $\text{RuTe}_2$ . Table 1 summarizes the results.

The pyrometric observation on a  $\text{RuTe}_2$  sample heated in the Knudsen cell revealed the appearance of a black spot within the focussed image of the cell orifice at 1156 °C. The wobbling black spot was seen to disappear in a short while due to fast evaporation of Te under the reduced pressure. The black spot appearance could be repeated with a fresh sample every time notwithstanding the orifice image was having a foggy view due to high Te vapor formation. The observation suggests that the intermetallic compound undergoes melting at 1156 °C, though it is difficult to say whether the melting occurred congruently or incongruently. The melting temperature of 1156 °C was obtained with an overall uncertainty of  $\pm 10$  °C after correction of the window transmittance that changed by Te vapor coating during the pyrometric observation. XRD result of the heated sample showed the presence of Ru(s) phase only. The

Table 1  
Summary of phase transformations observed in Ru–Te binary

Transformation type	Composition ( $x_{\text{Te}}$ )	Temperature (°C)
$\text{Te(s)} \leftrightarrow \text{Te(l)}$	1.00	449( $\pm 0.5$ ) (melting)
$\text{RuTe}_2\text{(s)} + \text{Te(s)} \leftrightarrow \text{Te(Ru)(s)}$	0.987	433( $\pm 1$ ) (solvus)
$\text{Te(Ru)(s)} \leftrightarrow \text{Liq.}$		448( $\pm 0.5$ ) (melting)
$\text{RuTe}_2\text{(s)} + \text{Te(s)} \leftrightarrow \text{Te(Ru)(s)}$	0.969	435( $\pm 1$ ) (solvus)
$\text{Te(Ru)(s)} \leftrightarrow \text{Liq.}$		447( $\pm 0.5$ ) (melting)
$\text{RuTe}_2\text{(s)} + \text{Te(s)} \leftrightarrow \text{L}_2 + \text{Te(Ru)(s)}$	0.940	444( $\pm 1$ ) (eutectic)
$\text{Te(Ru)(s)} \leftrightarrow \text{Liq.}$		446( $\pm 1$ ) (melting)
$\text{RuTe}_2\text{(s)} + \text{Te(s)} \leftrightarrow \text{L}_2$	0.918	444( $\pm 0.5$ ) (eutectic)
$\text{RuTe}_2\text{(s)} + \text{Te(s)} \leftrightarrow \text{L}_2$	0.900	445( $\pm 1$ ) (eutectic)
$\text{RuTe}_2\text{(s)} + \text{L}_2 \leftrightarrow \text{L}_1$		447( $\pm 1$ ) (monotectic)
$\text{L}_1 + \text{L}_2 \leftrightarrow \text{Liq}$		450( $\pm 0.5$ ) (melting)
$m\text{-RuTe}_2\text{(s)} \leftrightarrow p\text{-RuTe}_2\text{(s)}$	0.800	439( $\pm 1$ ) (transformation)
$\text{RuTe}_2\text{(s)} + \text{Te(s)} \leftrightarrow \text{L}_2$		444( $\pm 1$ ) (eutectic)
$\text{RuTe}_2\text{(s)} + \text{L}_2 \leftrightarrow \text{L}_1$		448( $\pm 1$ ) (monotectic)
$\text{L}_1 + \text{L}_2 \leftrightarrow \text{Liq}$		452( $\pm 0.5$ ) (melting)
$m\text{-RuTe}_2\text{(s)} \leftrightarrow p\text{-RuTe}_2\text{(s)}$	0.750	439( $\pm 1.5$ ) (transformation)
$\text{RuTe}_2\text{(s)} + \text{Te(s)} \leftrightarrow \text{L}_2$		444( $\pm 1$ ) (eutectic)
$\text{RuTe}_2\text{(s)} + \text{L}_2 \leftrightarrow \text{L}_1$		447( $\pm 1$ ) (monotectic)
$\text{L}_1 + \text{L}_2 \leftrightarrow \text{Liq}$		450( $\pm 0.5$ ) (melting)
$m\text{-RuTe}_2\text{(s)} \leftrightarrow p\text{-RuTe}_2\text{(s)}$	0.700	439(1) (transformation)
$\text{RuTe}_2\text{(s)} + \text{Te(s)} \leftrightarrow \text{L}_2$		444( $\pm 1$ ) (eutectic)
$\text{RuTe}_2\text{(s)} + \text{L}_2 \leftrightarrow \text{L}_1$		446( $\pm 1$ ) (monotectic)

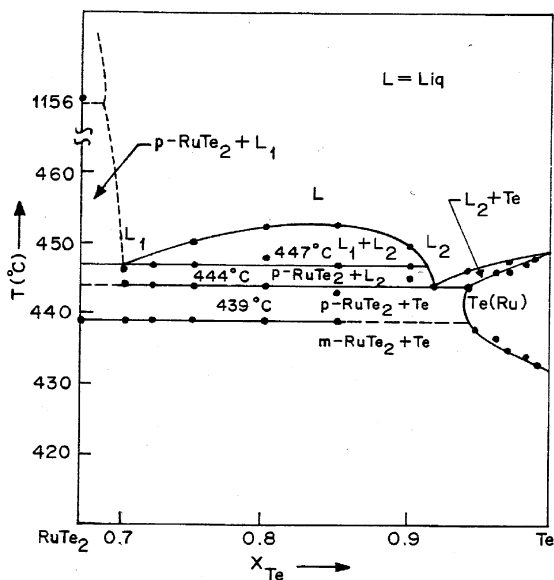


Fig. 3. The Ru–Te phase diagram from this study.

results of thermal and pyrometric studies led to the composition versus temperature diagram for the RuTe<sub>2</sub>–Te region of the Ru–Te binary system as shown in Fig. 3.

XRD analysis of a quenched sample of a composition  $x_{\text{Te}} = 0.80$  did not reveal the presence of the high-temperature liquid phases; XRD lines due to crystalline *p*-RuTe<sub>2</sub> and Te were seen instead. The absence of high-temperature phases in quenched samples could be due to their faster transformation to the solid phases.

#### 4. Discussion

It is seen in Fig. 3 that the Te-rich end ( $0.67 \leq x_{\text{Te}} \leq 1.00$ ) of the Ru–Te phase diagram arrived through the present study joins seamlessly to the results of the study reported for  $0.00 \leq x_{\text{Te}} \leq 0.68$  of the phase diagram [7]. Considering the reported result it is to be noted that RuTe<sub>2</sub> shown in the figure has a small homogeneity range between 67.3 and 67.8 at.% Te.

The pyrometrically observed melting of the intermetallic phase at  $(1156 \pm 10)$  °C could be corroborated to the observation reported in [7] that an endothermic peak was observed in DTA at  $(1175 \pm 1)$  °C. The temperature difference of 20 °C could be due to the uncertainty involved in this work and the reported study [7], both of which were carried out under high Te vapor. According to the available thermodynamic data [11], the RuTe<sub>2</sub>(s) + Ru(s) mixture attains Te<sub>2</sub>-pressure of 0.45 bar at 1175 °C and at this pressure it is expected to interfere in pyrometry as well as in the thermo emf measurements that are respectively used in the two studies.

The presence of monotectic phase field in the Te rich side of the intermetallic compound RuTe<sub>2</sub> as arrived

through the thermal analysis was suggested by Svendsen [12] from his analysis of measured vapor pressure over Te(l) saturated with RuTe<sub>2</sub>(s) in the temperature interval of 1003–1149 °C. The analysis showed that the Te activity corroborates to a small positive value of the partial molar enthalpy of the component in the liquid. The positive enthalpy was indicative of the formation of two liquids in the Te rich phase field at lower temperatures.

The crystallographic transition temperature at 439 °C arrived from thermal analysis of samples with  $x_{\text{Te}} = 0.667$ –0.800 agrees well with the reported value [7]. For samples with Te contents higher than  $x_{\text{Te}} = 0.85$ , the above transition could not be observed in the DTA; higher Te contents possibly impede on the kinetics of the crystallographic transition. The kinetic impedance is indicative of the monotropic transition noted in the reported study [7].

#### 5. Conclusion

The Ru–Te binary system is found to have a monotectic transformation at  $(447 \pm 1)$  °C at a composition of  $x_{\text{Te}} = 0.700$  and a eutectic transformation at  $(444 \pm 0.5)$  °C at a composition of  $x_{\text{Te}} = 0.918$ . Up to 6 at.% Ru is soluble in Te at about 440 °C.

#### Acknowledgement

The authors thank Shri A.N. Shirsat for his help during sample preparation and carrying out of the experiments.

#### References

- [1] H. Kleykamp, J. Nucl. Mater. 131 (1985) 221.
- [2] H. Kleykamp, J. Nucl. Mater. 206 (1993) 82.
- [3] H. Kleykamp, Nucl. Technol. 80 (1988) 412.
- [4] L. Thomassen, Z. Phys. Chem. B 2 (1929) 349.
- [5] H. Zhao, H.W. Schils, C.J. Raub, J. Less-Common Met. 86 (1982) L13.
- [6] H. Zhao, H.W. Schils, C.J. Raub, J. Less-Common Met. 113 (1985) 75.
- [7] S. Bernath, H. Kleykamp, W. Smykatz-Kloss, J. Nucl. Mater. 209 (1994) 128.
- [8] R. Mishra, P.N. Nambodiri, S.N. Tripathi, S.R. Dharwadkar, J. Alloys Comp. 280 (1998) 56.
- [9] S.P. Garg, Y.J. Bhatt, R. Venkataramani, Mater. Sci. Forum. 3 (1985) 419.
- [10] J.F. Schooley (Ed.), Temperature – its Measurement and Control in Science and Industry, Part 1, vol. 6, American Institute of Physics, New York, 1992, p. 373.
- [11] M. Ali (Basu), A.N. Shirsat, R. Mishra, A.S. Kerkar, S.C. Kumar, S.R. Bharadwaj, D. Das, J. Alloys Comp. 352 (2003) 140.
- [12] S.R. Svendsen, J. Chem. Thermodyn. 9 (1977) 789.